

Indoor Channel Spectral Statistics, K-factor and Reverberation Distance

Yochay Lustmann and Dana Porrat

School of Engineering and Computer Science, The Hebrew University, Jerusalem, Israel

Abstract—The frequency (spectral) statistics of the line of sight channel is adequately described by the Rice distribution. The Ricean K-factor is extracted from a large body of measurements; it is given against terminal separation and carrier frequency in the range 2–18 GHz. A model based on a power law of the terminal separation and the reverberation distance is suggested. The electromagnetic reverberation distance is characterized for two different rooms, it is bigger for the larger room and tends to increase with frequency. The non line of sight spectral and spatial statistics are similar to each other and characterized by the Rayleigh distribution.

Index Terms—Electromagnetic propagation, Indoor radio communication, Multipath channels.

I. INTRODUCTION

INDOOR radio propagation enjoys renewed interest due to extensive research of sensor networks, that have applications for entertainment, surveillance, telemedicine and environmental monitoring. Of particular interest in channel characterization is the line of sight (LoS) scenario, where communicating nodes enjoy a high quality link.

Radio system design generally relies on models of the propagation environment in the expected areas of deployment. Realistic channel models are needed for a fair comparison of algorithms and parameters during the design process, and for comparing the performance of different radio system.

It is generally accepted that line of sight propagation is characterized by the Rice distribution, but a systematic description of the distribution parameters in indoor setting has not been available until now in the public domain literature. This paper quantitatively characterizes the propagation channel in two rooms. We give a simple model of the Ricean K-factor vs. carrier frequency and transmitter–receiver separation. The results span the 2–18 GHz band, encompassing frequencies currently used for cellular and cordless telephones, the Wifi (IEEE 802.11) and Wimax (IEEE 802.16) standards, the entire UWB band, and higher frequencies that may be occupied by future radio systems.

With line of sight available between transmitter and receiver, the power received over the direct path follows the free space model. The main cause for received signal distortion are the multipath, i.e. the diffuse component of the channel. The signal carried over the diffuse component is typically much stronger than the additive noise and interference. The Ricean K-factor equals the ratio of power received over the direct path to the diffuse power and thus characterizes the multipath.

This research was supported by The Israel Science Foundation (Grant No. 249/06) and the Israeli Short Range Consortium (ISRC).

Measurements of the K-factor with results between 0 and 7 are reported by a number of papers: [1] measured values of up to 7 at 5.2 GHz, depending on the number of pedestrians in the vicinity of the system. Results from about 2 to 5 at frequencies of 2.4 GHz and 2.6 GHz are given by [2] and [3], note that the setup described in [3] had the two antennas very close to one wall.

Collecting significant channel statistics in the spatial domain is difficult because the statistics depend on terminal separation. A spectral-spatial analysis of the Ricean K-factor (i.e. averages over the two dimensions) in [3] was performed over sections shorter than 5 wavelengths of the center frequency, and the authors comment that this choice of area was done empirically, so that the received power over it would not change significantly.

This work presents statistics in the spectral domain, in bands of 2 GHz between 2 GHz and 18 GHz. The similarity of the spatial and the spectral statistics is demonstrated in non light of sight (NLoS) settings, where meaningful spatial statistics can be easily collected.

We characterize the dependence of the K-factor on carrier frequency and on transmitter–receiver separation using the *reverberation distance* [4], also called *critical distance* [5], a concept taken from the field of acoustics. The reverberation distance R_d is defined as the distance from the transmitter where the direct component is as strong as the diffuse component of the channel response. For a Rice–distributed channel the reverberation distance equals the distance where the K-factor equals one.

II. MEASUREMENT ENVIRONMENT AND EQUIPMENT

A. The System

The setup was based on an Agilent N5230 network analyzer (NA), connected to two omni-directional antennas (Electro-Metrics EM-6865). The network analyzer transmitted sinusoidal waves in the 2-18 GHz band with a frequency step of 1.06 MHz.

Each frequency was transmitted for about 0.02 seconds (the reciprocal of the NA intermediate frequency bandwidth), and the relative amplitude and phase, compared to the transmitted signal, were recorded. The SNR of all our LoS measurements was higher than 34 dB. The coherence bandwidth for the LoS phase measurements was between 25 to 85 MHz.

The receive antenna (Rx) was placed on a motorized positioner with sub-millimeter accuracy, that was one meter long and 20 cm wide. The receiver moved between measurements but was

kept immobile during the collection of each channel response. The transmit antenna (Tx) was placed on a cart that was moved to different locations for different measurements, but was immobile during each measurement. Tx and Rx antennas were both maintained 1.25 m above the floor.

A computer controlled the location of the receive antenna along the rail, as well as the parameters of the network analyzer and the data collection and management.

Measurements were normally performed during nights, when movement of people around the system was minimal.

B. Calibration

We used a Line of Sight (LoS) measurement with about 45 cm between receiver and transmitter antennas to calibrate the system. The radiation pattern of a biconical antenna is similar to that of a short dipole [6], and its far field boundary is thus about $\frac{\lambda}{2}$, below the calibration distance of 45 cm over the entire measurement band. This calibration method allows to calibrate out the cable and antenna responses but has the disadvantage of including multipath components. In order to overcome this difficulty we transformed the calibration measurement to the time domain using a rectangular window, cut out the multipath components (by eliminating the small amplitudes that come after the main pulse), and transformed it back to the frequency domain. We got a calibration response that can be used as follows:

$$r_f = \frac{r_f^{(measurement)}}{r_f^{(calibration)}} \quad (1)$$

$$\phi_f = \phi_f^{(measurement)} - \phi_f^{(calibration)} \quad (2)$$

Where r_f is the amplitude and ϕ_f is the phase for the frequency f .

The distance between Tx and Rx during calibration is denoted R_{Cal} , and after the calibration process we consider each transmitted sinusoidal wave as if it had amplitude 1 and phase 0 at distance R_{Cal} from the transmitter.

C. The Measurement Environment

The measurements used in this paper were collected in 2008-2009 in the Ross building at Givat Ram campus of the Hebrew University of Jerusalem. We measured in LoS and Non Line of Sight (NLoS) conditions. The LoS measurements were performed in two office rooms:

- 1) Big room. $9.5 \times 6.5 \times 2.6$ m³, about 12,000 measurements with 47 different cart (Tx) and motorized rail (Rx) positions.
- 2) Small room. $4 \times 3.5 \times 2.1$ m³, about 2,300 measurements with 8 different cart and motorized rail positions.

III. SPATIAL AND SPECTRAL STATISTICS

The statistical description of the radio channel, given small-scale fading conditions, is often modeled by the Rice or Rayleigh distributions. The Rice distribution is used in the presence of a dominant component (as common in LoS conditions) and the Rayleigh is typical when there is no dominant

component (common in NLoS conditions).

Observing the small-scale fading statistics can be done by sampling the amplitudes and phases of a narrow band signal in an area that is no bigger than a few times the wavelength. In this paper we refer to this as *spatial statistics*. The small-scale fading phenomenon can also be observed looking at the amplitude and phase distribution of the harmonic components of the channel. We refer to this as *spectral statistics*. The assumption of identical statistics in the spatial and spectral domains is in fact an assumption of ergodicity, related to the time-frequency ergodicity mentioned by [7]. The LoS channel between sets of directional antennas was found non-ergodic by [8], note that the results there are based on only ten spatial measurements, and that the existence of a line of sight depended strongly on the orientation of hand-held devices.

The Rice and Rayleigh distributions can be used to model the small-scale spectral statistics, as shown in Section IV-B, and it is natural to assume that the same statistics apply in the spatial domain.

We demonstrate in Section III-B that spatial and spectral statistics of NLoS channel measurements are similar.

With a dominant component (as in LoS), the small-scale spatial statistics is not easy to measure because the dominant component itself can change significantly within the sampling area. This causes difficulty because the Rice model assumes a constant dominant component. For spectral statistics this problem does not exist and observing the Rice statistics is simple.

We continue with the assumption that the spatial and spectral statistics of the small scale fading are identical also in LoS conditions, so the ability to extract the spectral distribution parameters gives information on the same parameters in space. In other words, we extract the K-factor of the Rice distribution using wideband spectral measurements, and assume it is the same for spatial statistics.

A. NLoS Measurements and Analysis

For NLoS conditions there is no dominant component, so observing the statistics of the amplitude is simple for both spatial and spectral measurements. In order to test the similarity between the two statistics the following set of measurements was performed:

- 1) **NLoS spatial measurements:** The transmitter and the receiver were placed in different rooms of the same building. The receiver moved on a 100×20 cm² rectangle using a motorized positioner with 4 mm steps (total of 12,801 positions). In each position the frequencies $f_c = 3, 6, \dots, 17$ GHz were transmitted and the channel response was measured.
NLoS spatial analysis: For each frequency (f_c) the mean and the variance of the channel's amplitude were extracted (see Figure 1).
- 2) **NLoS spectral measurements:** Without moving the transmitter or the receiver cart, nine additional measurements were taken in the corners and in the middle of the 100×20 cm² rectangle. The measurements were taken with a 1.06 MHz spectral step over the 2 - 18 GHz band.

NLoS spectral analysis: For the nine measurements the mean and the variance of the channel's amplitude for 2 GHz bands (2 - 4, 3 - 5 ... 16 - 18 GHz) were extracted. In Figure 1 the average (over the nine measurements) of the mean and variance is presented versus the center frequency (f_c) of each 2 GHz band.

B. NLoS Ergodicity Results

The moments of the channel's response calculated over space and over the spectrum can now be compared, as presented in Figure 1. The resemblance between the two is apparent, except for the low frequencies (3 - 5 GHz) where the wavelength ($\lambda \approx 6 - 10$ cm) was probably too large to give adequate spatial statistics on the 100×20 cm² area. We performed similar NLoS measurements at two other rooms, and got similar resemblance for the mean and variance of the amplitude distributions in the spatial and spectral measurements¹.

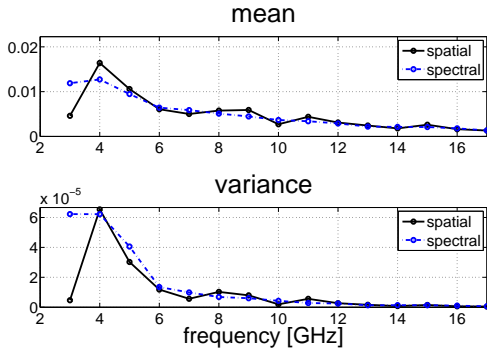


Fig. 1. Mean and variance of the amplitude of the NLoS measurements. In solid line the spatial measurements, and in dashed line the average of the nine spectral measurements.

IV. ANALYSIS

A. Measured Channel Phase

Assuming free space (FS) conditions, the calibrated channel response is given by:

$$\psi_f^{(FS)}(t) = A(T) \cos(2\pi ft + \phi_f(T)) \quad (3)$$

$$\phi_f(T) = -2\pi fT \quad (4)$$

$$A(T) = \frac{R_{cal}}{Tc_0 + R_{cal}} = \frac{R_{cal}}{R} \quad (5)$$

Where f is the frequency of the sinusoidal wave, t is the time, c_0 is the speed of light, R_{cal} is the distance between Tx and Rx antenna for the calibration measurement, R is the distance between Tx and Rx antenna for the measurement and T is a propagation delay that corresponds to $R - R_{cal}$.

In phasor representation we have

$$\psi_f^{(FS)} = A(T)e^{i\phi_f(T)} \quad (6)$$

Knowing that our receiver and transmitter are at fixed points during the measurement, we choose with no further loss of generality $\phi_f(T) = 0$ and denote $A(T)$ as A :

$$\psi_f^{(FS)} = A \quad (7)$$

Taking into account realistic LoS office conditions, the sinusoidal wave detected at the receiver is the sum of the free space signal and a diffuse component:

$$\psi_f = A + \tilde{r}_f e^{i\theta_f} \quad (8)$$

Where \tilde{r}_f is a random amplitude and θ_f is a random phase. Notice that the diffuse component $\tilde{r}_f e^{i\theta_f}$ is a superposition of all the multipath components, apart from the direct one.

Now we can associate ψ_f with the measured amplitude r_f , and with the phase deviation from free space $\Delta\phi_f$ (see Figure 2):

$$r_f = |\psi_f| \quad (9)$$

$$\Delta\phi_f = \arg(\psi_f) \quad (10)$$

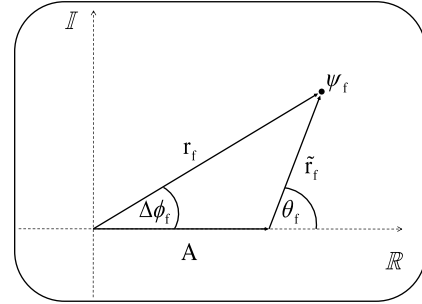


Fig. 2. ψ_f on the complex plane. A is the deterministic free space amplitude of the channel. \tilde{r}_f is a random amplitude caused by the multipath components, that has a random phase θ_f . r_f is the amplitude we measure and $\Delta\phi_f$ is the phase deviation of the measured channel from free space.

In Figure 3, a LoS measurement of ψ is demonstrated.

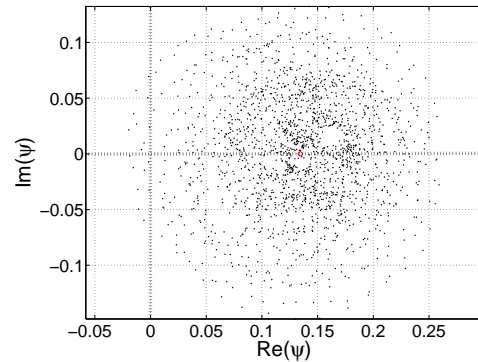


Fig. 3. Example of the calibrated channel response on the complex plane taken from a LoS measurement of about $R = 287.5$ cm with center frequency $f_0 = 9$ GHz and bandwidth 2 GHz. Each black dot represents ψ_f measured at a different frequency.

¹again we found some discrepancies for the low frequencies.

Measuring the amplitude (r_f) is straightforward and given directly by the NA as it measures the relation between received and transmitted amplitude at each frequency.

Measuring the phase deviation from free space ($\Delta\phi_f$) is not as simple because of the 2π modulus property. Still we can estimate $\Delta\hat{\phi}_f$ using the following algorithm:

- 1) Estimating the wave propagation time (\hat{T}):

We approximate \hat{T} with great accuracy by applying a Fourier transform on the data received from all frequencies (2 - 18 GHz), and looking for the peak position in the time domain²:

$$\hat{T} = \arg \max_t \left(\sum_f r_f \cos(2\pi ft + \phi_f) \right) \quad (11)$$

- 2) Simulating free space phase versus frequency using (4):

$$\hat{\phi}_f = \text{mod}(-2\pi f\hat{T}, 2\pi) \quad (12)$$

- 3) Subtracting the phase that was measured by the NA from the simulated one:

$$\Delta\hat{\phi}_f = \hat{\phi}_f - \phi_f \quad (13)$$

- 4) Modulus correction:

- a) If the value of the subtraction is bigger than π , 2π is subtracted from the result.
- b) If the value of the subtraction is smaller than $-\pi$, 2π is added to the result.

Of course, if the absolute actual phase deviation is bigger than π we will essentially get a random result for $\Delta\hat{\phi}_f$. This occurs under NLoS conditions, mainly because we cannot estimate the time of arrival properly.

Extraction of the phase deviation is illustrated in Figure 4, where $\Delta\hat{\phi}_f$ is the vertical distance on the graph between the measured black dots and the simulated solid line. In cases where the absolute vertical distance is bigger than π (around 7.125 GHz for example), a correction is needed because of the modulus property.

B. Statistical Models

1) *The Rice Distribution*: Assuming the number of multipath components is sufficiently large, we expect the central limit theorem to hold, so the distribution of $\tilde{r}e^{i\theta}$ should be almost normal on the complex plane. We can now describe the phase-amplitude joint distribution as a two dimensional Gaussian function, with diffuse parameter σ and radial symmetry around $(A, 0)$:

$$pdf(r, \Delta\phi) = \frac{r}{2\pi\sigma^2} e^{-\frac{(r \cos(\Delta\phi) - A)^2 + (r \sin(\Delta\phi))^2}{2\sigma^2}} \quad (14)$$

²In LoS room conditions we can estimate the time of arrival with a very high precision, usually less than 2 ps (much smaller than our shortest wave period of about 55 ps).

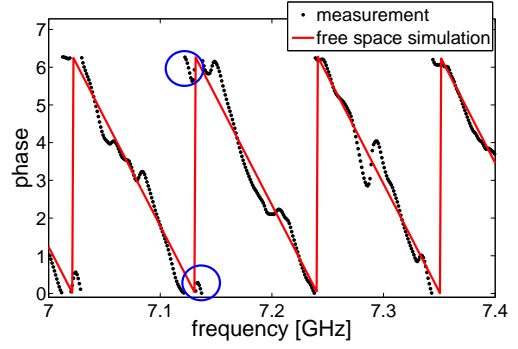


Fig. 4. Example of LoS measured phase versus frequency and an appropriate free space simulation according to equation (12). The estimated time of arrival (\hat{T}) for the simulation was calculated using equation (11). When extracting $\Delta\phi_f$ from the measurements in the circles a modulus correction is needed.

Equation (14) describes the phase-amplitude joint Rice distribution, where the amplitude and phase distribution can be extracted [9], [10]:

$$pdf_{Rice}(r) = \int_0^{2\pi} pdf(r, \Delta\phi) d\Delta\phi = \frac{r}{\sigma^2} e^{-\frac{r^2 + A^2}{2\sigma^2}} I_0\left(\frac{rA}{\sigma^2}\right); r > 0 \quad (15)$$

$$pdf_{\Delta\phi}(\Delta\phi) = \int_0^{\infty} pdf(r, \Delta\phi) dr = \frac{1 + \sqrt{\pi K} e^{K \cos^2(\Delta\phi)} \cos(\Delta\phi) \left[1 + \text{erf}\left(\sqrt{K} \cos(\Delta\phi)\right)\right]}{2\pi e^K} \quad (16)$$

$$K = \frac{A^2}{2\sigma^2} \quad (17)$$

Where K is the Ricean K-factor, $I_0(x)$ is the modified Bessel function of the first kind with order zero and $\text{erf}(x)$ is the error function:

$$\text{erf}(x) = \frac{2}{\sqrt{\pi}} \int_0^x e^{-z^2} dz \quad (18)$$

2) *The Rayleigh Distribution*: Given small-scale fading conditions without a dominant component (NLoS condition) we have $A=0$, so instead of (15) and (16) we have the Rayleigh distribution for the amplitude and a uniform circular distribution for the phase (notice that now we have $\Delta\phi = \theta$):

$$pdf_{Rayleigh}(r) = \frac{r}{\sigma^2} e^{-\frac{r^2}{2\sigma^2}}; r > 0 \quad (19)$$

$$pdf_{\theta}(\theta) = \frac{1}{2\pi} \quad (20)$$

Extracting the diffuse parameter σ for the Rayleigh distribution is done using the first moment of the amplitude (r):

$$\hat{\sigma} = \sqrt{\frac{2}{\pi}} \text{mean}(r) \quad (21)$$

C. Extracting the Ricean K-Factor

For the Rice distribution, the most common estimation method of the K-factor is based on the first two moments of the channel's power [11]. We found that for our measured data, the power-based method did not yield adequate results, and sometimes even returned complex numbers. We used our phase measurements in addition to the amplitude to extract the K-factor, and did it in two ways that gave similar results:

1) *Phase and Amplitude Method*: If we assume that θ_f is uniformly distributed, then using (8) the free space power (A^2) and the diffuse power ($2\sigma^2$) can be extracted simply by calculating the average and variance of ψ_f :

$$\hat{A}^2 = |\text{mean}(\psi_f)|^2 \quad (22)$$

$$2\hat{\sigma}^2 = \text{var}(\psi_f) \quad (23)$$

$$\hat{K} = \frac{\hat{A}^2}{2\hat{\sigma}^2} \quad (24)$$

Another way to extract A uses the time of arrival \hat{T} (11), as can be seen from (5). Figure 5 shows the estimates of A from measurements with $f_c = 7$ GHz.

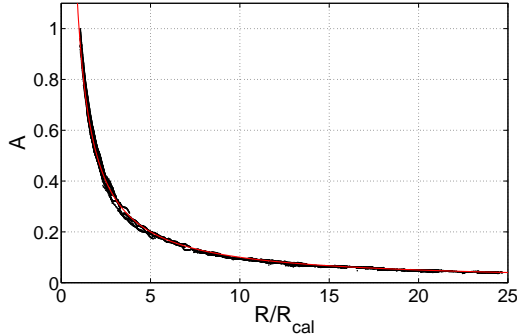


Fig. 5. Estimates of A using equation (22). The dots represent \hat{A} , taken from about 12,000 LoS measurements in the big room, with mean frequency $f_0 = 7$ GHz. The solid line represents $\frac{R_{\text{cal}}}{R}$ (Equation (5)). We got a good agreement also for the other frequencies.

2) *Phase Only Method*: Another way to extract the Ricean K-factor is by finding the standard deviation of $\Delta\phi$, denoted $\sigma_{\Delta\phi}$. As can be seen in (16), the pdf of the phase-deviation is a symmetric function that depends only on the Ricean K-factor, so a one to one relation between K and $\sigma_{\Delta\phi}$ can be found by calculating the standard deviation of equation (16) for different values of K . The Ricean K-factor can be extracted using a lookup table.

V. RESULTS

A. Statistical Model

1) *LoS*: For each LoS measurement we extracted the appropriate parameters of the Rice, Rayleigh, Nakagami and Log-Normal distributions for the amplitude, and the Von Mises, Wrapped Cauchy, Wrapped Laplace and Rice for the phase as described in Sections IV-B2, IV-C1 and Appendix A. The

Akaike Information Criterion (AIC) score was calculated for each statistical model as described in Appendix A-C, to test which model had the lowest score.

The results of about 14,500 measurements (taken with 55 different cart (Tx) and motorized rail (Rx) positions in the big and small rooms) are presented in Figure 6.

The Rice model best describes the phase distribution for all the frequencies. For the amplitude distribution, the Rice model is best for the 4 - 15 GHz band, and the Nakagami model has the best agreement for $f_c = 3$ and 16 - 17 GHz.

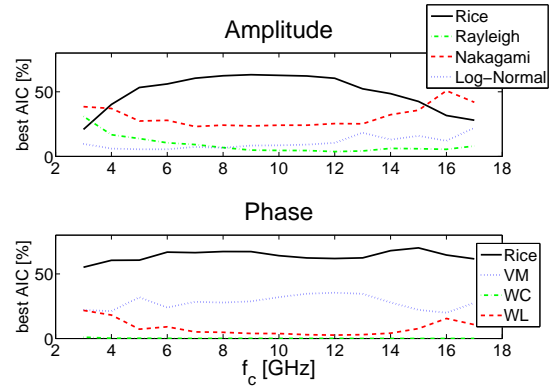


Fig. 6. Best statistical model for the LoS amplitude (r) and phase-deviation ($\Delta\phi$) spectral distribution. The bandwidth is 2 GHz. The Von Mises (VM), Wrapped Cauchy (WC) and Wrapped Laplace (WL) distributions are presented in Appendix A-A. The Nakagami and Log-Normal distributions are presented in Appendix A-B. The Rice distribution is superior over the entire band for the phase and over the band 4 - 15 GHz band for the amplitude. The Nakagami is better for $f_c = 3$ and 16 - 17 GHz.

2) *NLoS*: For almost all the NLoS measurements the Rayleigh distribution was superior to the Log-Normal one, i.e. it agreed better with the spectral and spatial histograms. The Log-Normal distribution agreed better with a single spatial histogram at $f_c = 3$ GHz, see Section III-B. In Figure 7 the histogram of one of the spectral measurements is presented together with its Rayleigh and Log-Normal curves.

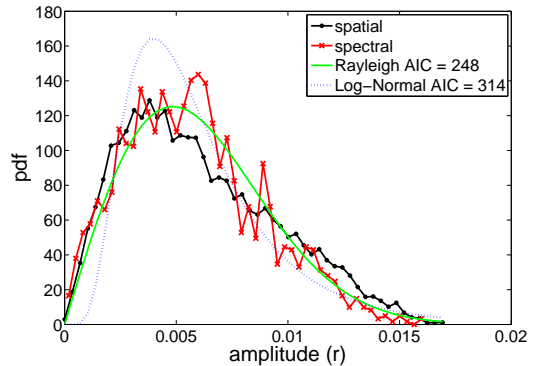


Fig. 7. Spatial and spectral amplitude histograms for a NLoS measurement with $f_c = 6$ GHz. As can be seen from Figure 1 the mean and variance for the 6 GHz spatial and spectral measurements are almost identical, so we have a good match between the histograms. The Rayleigh and Log-Normal curves for the spectral measurement are also shown.

B. K-Factor

From each LoS measurement we extracted the spectral K-factor in 2 GHz bands using the phase and amplitude method as described in Section IV-C1. The K-factor is presented in Figure 8 as a function of the spatial distance between transmitter and receiver (R), after averaging over bins of about 1 cm.

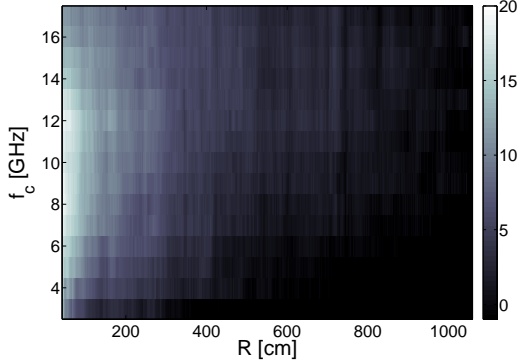


Fig. 8. About 12,000 LoS K-factor results (dB) over 2 GHz bands taken in the big room and averaged in steps of about 1 cm. The measurements were taken with 47 different cart (Tx) and motorized rail (Rx) positions. For the small room the pattern is similar.

Looking at the results in Figures 8 we conclude the following:

- 1) **Dependence on terminal separation.** The K-factor tends to decrease as the distance between transmitter and receiver increases. This behavior suggests that the deterministic LoS component (A) decreases faster than the diffuse component (σ).
- 2) **Dependence on center frequency.** For the low to medium frequencies ($f_c = 3 - 12$ GHz) the K-factor tends to increase as the center frequency increases. For the high frequencies ($f_c = 12 - 17$ GHz) the trend is reversed and the K-factor decreases with center frequency.

1) Modeling the K-Factor:

- 1) **An Empirical Model.** The K-factor results can be described by a power law model with frequency dependent scaling parameter $n(f)$ and reverberation distance $R_d(f)$:

$$K(R) = \left(\frac{R_d(f)}{R} \right)^{n(f)} \quad (25)$$

Table I lists the empirical values of the reverberation distance and the scaling parameter for the two rooms.

Figure 9 and Table I display the scaling parameter n for the big and small rooms. It seems that in the small room the decrease rate of K is usually higher than in the big room. This can also be explained by the stronger diffuse influence in the small room.

- 2) **A Simplified Model.** A simplified empirical model is applicable in the 3 - 12 GHz band:

$$K(f_c, R) = \left(\frac{\Theta f_c + \Omega}{R} \right)^n \quad (26)$$

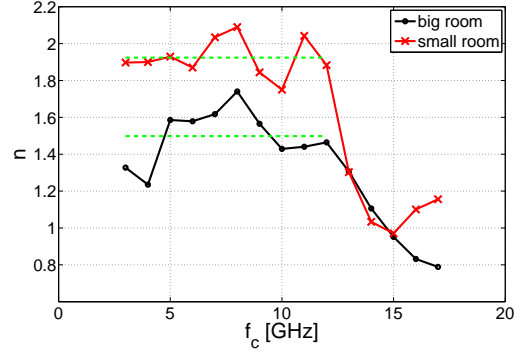


Fig. 9. The scaling parameter $n(f)$ extracted from the K-factor measurements using the model (25). The dashed lines are the average values over frequencies 3 - 12 GHz given in Table II.

f_c [GHz]	big room			small room		
	R_d [m]	n	RMS	R_d [m]	n	RMS
3	2.78	1.33	0.41	1.60	1.90	0.31
4	4.75	1.24	0.59	2.17	1.90	0.60
5	4.45	1.59	0.81	2.44	1.93	0.66
6	5.20	1.58	0.79	2.90	1.87	0.61
7	6.03	1.62	0.84	3.25	2.03	1.08
8	5.68	1.74	0.92	3.15	2.09	1.03
9	7.16	1.56	1.04	3.44	1.84	0.71
10	8.58	1.43	1.18	3.67	1.75	0.60
11	9.10	1.44	1.33	3.43	2.04	1.22
12	9.39	1.46	1.40	4.26	1.88	1.09
13	10.46	1.31	1.00	6.37	1.30	0.92
14	12.14	1.11	0.60	7.89	1.03	0.79
15	15.76	0.95	0.82	9.16	0.97	0.82
16	17.82	0.83	0.78	6.86	1.10	0.71
17	17.71	0.79	0.76	6.03	1.16	0.63

TABLE I
EXTRACTED REVERBERATION DISTANCE (R_d) AND SCALING PARAMETER (n) USING MATLAB 'FIT' TO EQUATION (25). f_c IS THE CENTER FREQUENCY OF THE 2 GHz BAND USED TO ESTIMATE THE RICEAN K-FACTOR. RMS IS THE ROOT MEAN SQUARE ERROR OF THE K-FACTOR MODEL.

Where Θ , Ω and n are parameters set to fit the results, and displayed in Table II. These parameters do not depend on frequency.

	$\Theta \left[\frac{m}{GHz} \right]$	$\Omega [m]$	n	RMS
big room	0.70	1.03	1.50	1.70
small room	0.25	1.19	1.92	1.71

TABLE II
PARAMETERS FOR THE SIMPLIFIED MODEL (26) EXTRACTED FROM K-FACTOR RESULTS USING THE MATLAB 'FIT' FUNCTION. RMS IS THE ROOT MEAN SQUARE ERROR BETWEEN THE K-FACTOR MODEL AND THE MEASURED RESULTS.

C. Reverberation Distance

Figure 10 and Table I show the estimated reverberation distance (R_d) for the big and small rooms as function of the center frequency (f_c). The reverberation distance in the small room is smaller. The dependence of R_d on the room's surface area (S) is given in [4]:

$$R_d \propto \sqrt{S} \quad (27)$$

Using the dimensions of the rooms, we have $S^{(big)} = 206.7 \text{ m}^2$ and $S^{(small)} = 59.5 \text{ m}^2$, so we can expect:

$$\frac{R_d^{(big)}}{R_d^{(small)}} = 1.86$$

This is close to the results in Figures 10 where the average ratio between the reverberation distances is 2.06, with a standard deviation of 0.4.

It is also clear from Figure 10 that the reverberation distance usually increases as the center frequency increases.

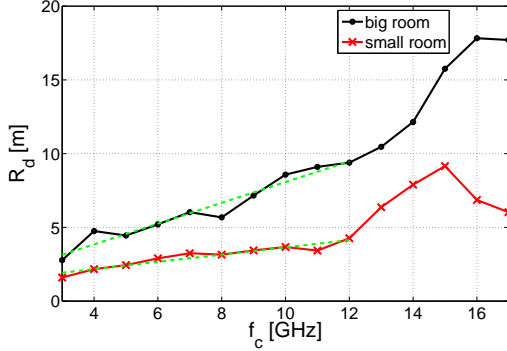


Fig. 10. The reverberation distance R_d as extracted from the K-factor measurements using the model from (25). The dashed lines represent $R_d = \Theta f_c + \Omega$, where Θ and Ω are as in Table II.

VI. CONCLUSION

Results from an extensive indoor line of sight measurement campaign in the frequency domain were presented. By extracting the spectral Ricean K-factor for different frequencies and terminal separation, an insight of the indoor multipath diffuse propagation and reverberation distance was given.

We found that the average K-factor depends on Tx-Rx distance (R) via a power law $K(R) = \left(\frac{R_d}{R}\right)^n$, where the reverberation distance (R_d) and scaling parameter (n) were extracted.

For the central frequency range of 3 - 12 GHz the scaling parameter (n) was approximately constant, and the reverberation distance (R_d) increased linearly with frequency. We assume the reverberation distance increase is due to low reflections from the walls for high frequencies, meaning weaker MPCs.

The reverberation distance was found to be larger in the bigger room. We attribute this difference to the weaker multipath components (MPCs) there. The direct path's power does not depend on room geometry or on frequency, but other MPCs travel larger distances in the bigger room, and are thus weaker there. Our results agree with a prediction of [4], namely reverberation distance values that are proportional to the square root of the room's surface area.

When testing the LoS spectral distribution we found that the Rice model best described the phase distribution for all frequencies, and best described the amplitude distribution for the frequency range of 4 - 15 GHz. In the 2 GHz bands around 3 and 16 - 17 GHz the Nakagami distribution was found to best describe the amplitude distribution.

For the spectral and spatial NLoS distribution we found the

Rayleigh model to best describe almost all of the measurements.

The spatial-spectral distribution ergodicity assumption was justified using NLoS measurements, where the mean and variance of the amplitudes were found to be similar.

To summarize the contributions:

- A simple model of the Ricean K-factor that depends on the carrier frequency and on the terminal separation.
- A characterization of the electromagnetic reverberation distance in the 3–17 GHz band.
- The spectral statistics of indoor channels are described by the Rayleigh and Rice distributions in the 2–18 GHz band, with other distributions (Nakagami and Log-Normal) sometimes suitable in the low and high ends of the band.
- A demonstration of the similarity of the spatial and spectral statistics of the channel in NLoS conditions.

APPENDIX A

COMPARISON OF PROBABILITY MODELS

A. Phase Distribution Models

In order to validate our statistical model for the phase distribution (16) we tested it against three known circular probability density functions:

- 1) Von Mises (VM) - also known as the circular normal distribution [12]:

$$pdf_{VM}(\Delta\phi) = \frac{1}{2\pi I_0(\kappa)} e^{\kappa \cos(\Delta\phi)} \quad (28)$$

where $I_0(x)$ is the modified Bessel function of order 0.

- 2) Wrapped Cauchy (WC) [12]:

$$pdf_{WC}(\Delta\phi) = \frac{1}{2\pi} \frac{1 - \rho^2}{1 + \rho^2 - 2\rho \cos(\Delta\phi)} \quad (29)$$

- 3) Wrapped Laplace (WL) [13]:

$$pdf_{WL}(\Delta\phi) = \frac{\gamma}{2} \frac{e^{2\pi - \Delta\phi} + e^{\gamma\Delta\phi}}{e^{2\pi\gamma} - 1} \quad (30)$$

Where κ , ρ and γ are parameters that were extracted using a lookup table against $\sigma_{\Delta\phi}$.

B. Amplitude Distribution Models

For the amplitude distribution we compared the Rice distribution (15) with the Rayleigh distribution (19), the Nakagami distribution and the Log-Normal distribution, all known to describe the statistics of multipath fading channels:

- 1) Nakagami:

$$pdf_{Nakagami}(r) = \frac{2\mu^\mu}{\Gamma(\mu)\omega^\mu} r^{2\mu-1} e^{-\frac{\mu}{\omega}r^2} \quad (31)$$

where $\Gamma(x)$ is the Gamma function.

- 2) Log-Normal:

$$pdf_{Log-Normal}(r) = \frac{1}{\delta\sqrt{2\pi}r} e^{-\frac{(\ln(r)-\eta)^2}{2\delta^2}} \quad (32)$$

Where μ , ω , δ and η are parameters that were extracted as follows:

- 1) For the Nakagami distributions the simplest parameters estimation method is based on the first two moments of the received signal power [10]:

$$\hat{\omega} = \text{mean}(r^2) \quad (33)$$

$$\hat{\mu} = \frac{\hat{\omega}^2}{\text{var}(r^2)} \quad (34)$$

As in the Rice distribution case, we found that for our measured data this method did not always give adequate results. In order to improve the parameters extraction we used our estimate of the Ricean K-factor:

$$\hat{\mu} = \frac{(\hat{K} + 1)^2}{2\hat{K} + 1} \quad (35)$$

$$\hat{\omega} = \hat{\mu} \left(\text{mean}(r) \cdot \frac{\Gamma(\hat{\mu})}{\Gamma(\hat{\mu} + \frac{1}{2})} \right)^2 \quad (36)$$

Notice that for NLoS measurements $A = 0$, so according to (17) and (35) we have $K = 0$ and $\mu = 1$. Under these conditions, the Rice and Nakagami distributions coincide with Rayleigh [9].

- 2) For the Log-Normal distribution, parameters estimation using the first two moments of the received amplitudes was found adequate [14]:

$$\hat{\delta} = \sqrt{\ln \left(1 + \frac{\text{var}(r)}{\text{mean}^2(r)} \right)} \quad (37)$$

$$\hat{\eta} = \ln(\text{mean}(r)) - \frac{1}{2}\hat{\delta}^2 \quad (38)$$

C. The Akaike Information Criterion (AIC)

In order to examine which probability model best fits our measurements, the Akaike information criterion (AIC), presented by [15] and popularized by [16], was used:

$$AIC = 2q + k \ln \left(\frac{\sum_{i=1}^k [y_i - f(x_i)]^2}{k} \right) \quad (39)$$

Where y_i denotes the histogram of the measured data, $f(x_i)$ the pdf of the statistical model, k is the number of bins in the histogram and q is the number of parameters in the statistical model. As described by [16], the AIC is an approximately unbiased estimator of the expected discrepancy, or distance, between probability density functions.

ACKNOWLEDGMENT

The authors thank Prof. Andy Molisch for his helpful comments and useful references.

REFERENCES

- [1] K. I. Ziri-Castro, N. E. Evans, and W. G. Scanlon, "Propagation modelling and measurements in a populated indoor environment at 5.2GHz," in *2006 Auswireless Conference*, 2006.
- [2] V. Nikolopoulos, M. Fiocco, S. Stavrou, and S. Saunders, "Narrowband fading analysis of indoor distributed antenna systems," *Antennas and Wireless Propagation Letters, IEEE*, vol. 2, pp. 89–92, 2003.
- [3] S. Wyne, T. Santos, F. Tufvesson, and A. Molisch, "Channel measurements of an indoor office scenario for wireless sensor applications," in *Global Telecommunications Conference, 2007. GLOBECOM '07. IEEE*, Nov. 2007, pp. 3831–3836.
- [4] J. Andersen, J. Nielsen, G. Pedersen, G. Bauch, and M. Herdin, "Room electromagnetics," *Antennas and Propagation Magazine, IEEE*, vol. 49, no. 2, pp. 27–33, April 2007.
- [5] J. J. Jetzt, "Critical distance measurement of rooms from the sound energy spectral response," *The Journal of the Acoustical Society of America*, vol. 61, no. S1, pp. S34–S34, 1977. [Online]. Available: <http://link.aip.org/link/?JAS/61/S34/3>
- [6] D. Ghosh and T. K. Sarkar, "Design of a wide-angle biconical antenna for wideband communications," *Progress In Electromagnetics Research B*, vol. 16, pp. 229–245, 2009.
- [7] R. Kattenbach and H. Fruchting, "Wideband measurements of channel characteristics in deterministic indoor environment at 1.8 GHz and 5.2 GHz," in *Personal, Indoor and Mobile Radio Communications, 1995. PIMRC'95. 'Wireless: Merging onto the Information Superhighway', Sixth IEEE International Symposium on*, vol. 3, Sep 1995, pp. 1166–1170.
- [8] J. Karedal, A. Johansson, F. Tufvesson, and A. Molisch, "A measurement-based fading model for wireless personal area networks," *Wireless Communications, IEEE Transactions on*, vol. 7, no. 11, pp. 4575–4585, November 2008.
- [9] M. Yacoub, G. Fraidenraich, and J. Santos Filho, "Nakagami-m phase-envelope joint distribution," *Electronics Letters*, vol. 41, no. 5, pp. 259–261, March 2005.
- [10] A. F. Molisch, *Wireless Communication*. John Wiley and Sons Ltd, 2005.
- [11] L. Greenstein, D. Michelson, and V. Erceg, "Moment-method estimation of the ricean k-factor," *Communications Letters, IEEE*, vol. 3, no. 6, pp. 175–176, Jun 1999.
- [12] S. R. Jammalamadaka and A. Sengupta, *Topics in Circular Statistics*. World Scientific, 2001.
- [13] S. R. Jammalamadaka and T. J. Kozubowski, "New families of wrapped distributions for modeling skew circular data," *Communications in statistics. Theory and methods*, vol. 33, no. 9, pp. 2059–2074, 2004.
- [14] E. Limpert, W. A. Stahel, and M. Abbt, "Log-normal distributions across the sciences: Keys and clues," *BioScience*, vol. 51, no. 5, pp. 341–352, May 2001.
- [15] H. Akaike, "A new look at the statistical model identification," *Automatic Control, IEEE Transactions on*, vol. 19, no. 6, pp. 716–723, Dec 1974.
- [16] U. Schuster and H. Bolcskei, "Ultrawideband channel modeling on the basis of information-theoretic criteria," *Wireless Communications, IEEE Transactions on*, vol. 6, no. 7, pp. 2464–2475, July 2007.